ARTICLE

Mutations of the Mitochondrial Holocytochrome *c*–Type Synthase in X-Linked Dominant Microphthalmia with Linear Skin Defects Syndrome

Isabella Wimplinger,* Manuela Morleo,* Georg Rosenberger, Daniela Iaconis, Ulrike Orth, Peter Meinecke, Israela Lerer, Andrea Ballabio, Andreas Gal, Brunella Franco, and Kerstin Kutsche

The microphthalmia with linear skin defects syndrome (MLS, or MIDAS) is an X-linked dominant male-lethal disorder almost invariably associated with segmental monosomy of the Xp22 region. In two female patients, from two families, with MLS and a normal karyotype, we identified heterozygous de novo point mutations—a missense mutation (p.R217C) and a nonsense mutation (p.R197X)—in the *HCCS* gene. *HCCS* encodes the mitochondrial holocytochrome *c*–type synthase that functions as heme lyase by covalently adding the prosthetic heme group to both apocytochrome *c* and c_1. We investigated a third family, displaying phenotypic variability, in which the mother and two of her daughters carry an 8.6-kb submicroscopic deletion encompassing part of the *HCCS* gene. Functional analysis demonstrates that both mutant proteins (R217C and Δ197–268) were unable to complement a *Saccharomyces cerevisiae* mutant deficient for the HCCS orthologue Cyc3p, in contrast to wild-type HCCS. Moreover, ectopically expressed HCCS wild-type and the R217C mutant protein are targeted to mitochondria in CHO-K1 cells, whereas the C-terminal–truncated Δ197–268 mutant failed to be sorted to mitochondria. Cytochrome *c,* the final product of holocytochrome *c*–type synthase activity, is implicated in both oxidative phosphorylation (OXPHOS) and apoptosis. We hypothesize that the inability of *HCCS*-deficient cells to undergo cytochrome *c*–mediated apoptosis may push cell death toward necrosis that gives rise to severe deterioration of the affected tissues. In summary, we suggest that disturbance of both OXPHOS and the balance between apoptosis and necrosis, as well as the X-inactivation pattern, may contribute to the variable phenotype observed in patients with MLS.

Microphthalmia with linear skin defects syndrome (MLS [MIM #309801]), also known as "MIDAS" (microphthalmia, dermal aplasia, and sclerocornea), is a rare X-linked dominant condition characterized by unilateral or bilateral microphthalmia and linear skin defects—which are limited to the face and neck, consisting of areas of aplastic skin that heal with age to form hyperpigmented areas—in affected females and in utero lethality for males. Additional features in female patients include agenesis of the corpus callosum, sclerocornea, chorioretinal abnormalities, infantile seizures, congenital heart defect, mental retardation, and diaphragmatic hernia.[1] In the majority of cases, patients carry a chromosomal aberration that results in segmental monosomy of the Xp22 chromosomal region (>11 Mb). To date, eight patients with an apparently normal female karyotype have been described.[2–6] The MLS minimal critical region has been delineated to 610 kb in Xp22.2, through breakpoint mapping of two X;Y translocations of patients not affected with MLS and of the smallest deletion characterized in a female with the typical MLS phenotype.[7] Three genes are located in the critical interval, including *MID1, HCCS,* and *ARHGAP6*[7] (fig. 1*A*). *MID1* is mutated in Opitz G/BBB syndrome,[8] whereas no disease-associated mutations have yet been described for *HCCS* and *ARHGAP6*. The *ARHGAP6* gene codes for a Rho GTPase–activating protein (Rho GAP) that functions as a GAP for the small GTPase RhoA, as well as a protein implicated in reorganization of the actin cytoskeleton.[9,10] *HCCS* encodes a mitochondrial holocytochrome *c*–type synthase, also known as "heme lyase," composed of 268 aa.[11,12] It catalyzes the covalent attachment of heme to both apocytochrome *c* and c_1, the precursor forms, thereby leading to the mature forms, holocytochrome *c* and c_1, which are necessary for proper functioning of the mitochondrial respiratory chain.[13,14] In addition to the well-known role of cytochrome *c* in oxidative phosphorylation (OXPHOS), cytochrome *c* is released from mitochondria in response to a variety of intrinsic death-promoting stimuli that, in turn, result in caspase-dependent cell death, namely "apoptosis."[15]

The majority of patients display the classic phenotypic features of MLS; however, a high intra- as well as interfamilial clinical variability that is not correlated with the extent of the chromosomal deletion has been reported. For example, a few patients show the typical skin defects but no ocular manifestation,[2,16–18] whereas others present

From the Institut für Humangenetik, Universitätsklinikum Hamburg-Eppendorf (I.W.; G.R.; U.O.; A.G.; K.K.), and Abteilung für Medizinische Genetik, Altonaer Kinderkrankenhaus (P.M.), Hamburg; Telethon Institute of Genetics and Medicine (M.M.; D.I.; A.B.; B.F.) and Medical Genetics, Department of Pediatrics, Federico II University (A.B.; B.F.), Naples, Italy; and Department of Human Genetics, Hadassah Hebrew University Hospital, Jerusalem (I.L.)

Received July 24, 2006; accepted for publication August 15, 2006; electronically published September 6, 2006.

Address for correspondence and reprints: Dr. Kerstin Kutsche, Institut für Humangenetik, Universitätsklinikum Hamburg-Eppendorf, Butenfeld 42, D-22529 Hamburg, Germany. E-mail: kkutsche@uke.uni-hamburg.de

* These two authors contributed equally to this work.

Am. J. Hum. Genet. 2006;79:878–889. 0002-9297/2006/7905-0010$15.00

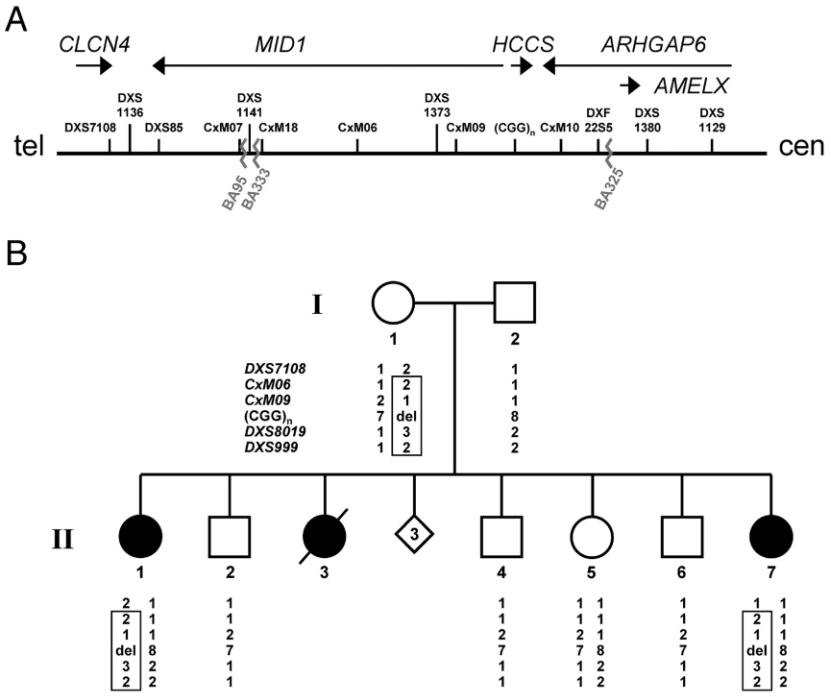

Figure 1. Minimal MLS critical region and haplotype analysis of the family of patient II.7. *A,* Schematic representation of the minimal MLS critical region (610 kb) in Xp22.2, defined by the breakpoints of patients BA333 and BA325 (*jagged lines*). The figure is not drawn to scale. The uppermost arrows show the orientation of genes within the critical region. The position of DNA marker loci previously mapped in this region is shown. *B,* Haplotype analysis of six representative polymorphic markers in Xp22.2-p22.13 in the family of patient II.7. Whereas markers *DXS7108, CxM06, CxM09,* and SNP *rs5901444*—$(CGG)_n$—are positioned in the MLS critical region and indicated in panel A, loci *DXS8019* and *DXS999* are located centromeric to the critical region. The polymorphic $(CGG)_n$ repeat is located in the *HCCS* 5′ UTR, and the respective repeat length is given. Alleles are shown below the pedigree symbols. del = Deletion of one allele. The haplotype shared by the affected sisters (II.1 and II.7) and their mother (I.1) is boxed. Both patients II.7 and II.1 carry only the paternal allele, with eight CGG repeats, whereas the unaffected sister (II.5) is heterozygous for the trinucleotide repeat. Segregation analysis showed that the three brothers (II.2, II.4, and II.6) and the unaffected sister (II.5) carry a different maternal haplotype than do II.1 and II.7.

with only eye abnormalities, and dermal lesions are absent.[19–21] It has been suggested that the pattern of X inactivation may play a role in the development of the various symptoms seen in patients with MLS.[22,23]

The identification of the genetic defect for MLS has been hampered by the absence of patients with a full-blown MLS phenotype and a normal karyotype. In 2005, Morleo and colleagues[5] undertook the first attempt at a detailed characterization of four patients with MLS and no obvious chromosomal rearrangements. With use of FISH with genomic clones spanning the MLS critical region and a genomewide analysis with BAC microarrays, no microdeletion or duplication could be detected in these patients. Similarly, direct sequencing of coding regions and exon-intron boundaries of *MID1, HCCS,* and *ARHGAP6* revealed no pathogenic sequence alteration or small rearrangement that would suggest that these patients carry cryptic rearrangements that had been missed by the techniques applied.[5]

Material and Methods

Patients

We examined the family of proband II.7. She is the youngest daughter of healthy and unrelated parents. There is no maternal history of skin defect or any other pathology, nor is there any family history of genetic disease or malformations. The couple has three healthy sons and one healthy daughter. Three pregnancies ended with spontaneous abortions early in the first trimester (fig. 1*B*). The proband was born with a left anophthalmia, sclerocornea, and lateral skin defect on her cheek. At age 6 mo, she presented with junctional ectopic tachycardia, which was successfully treated by catheter ablation. At age 3 years, she had normal psychomotor development.

Her eldest sister (II.1) was born with the following manifestations: a left opaque cornea, congenital glaucoma with total anterior synechia, and a white anterior cataract. On the right side, she presented with corneal leukoma, which has resolved with time. She showed no other malformations, and her psychomotor development is normal. The couple had another baby girl, with bilateral anophthalmia, who died at age 6 h from complications

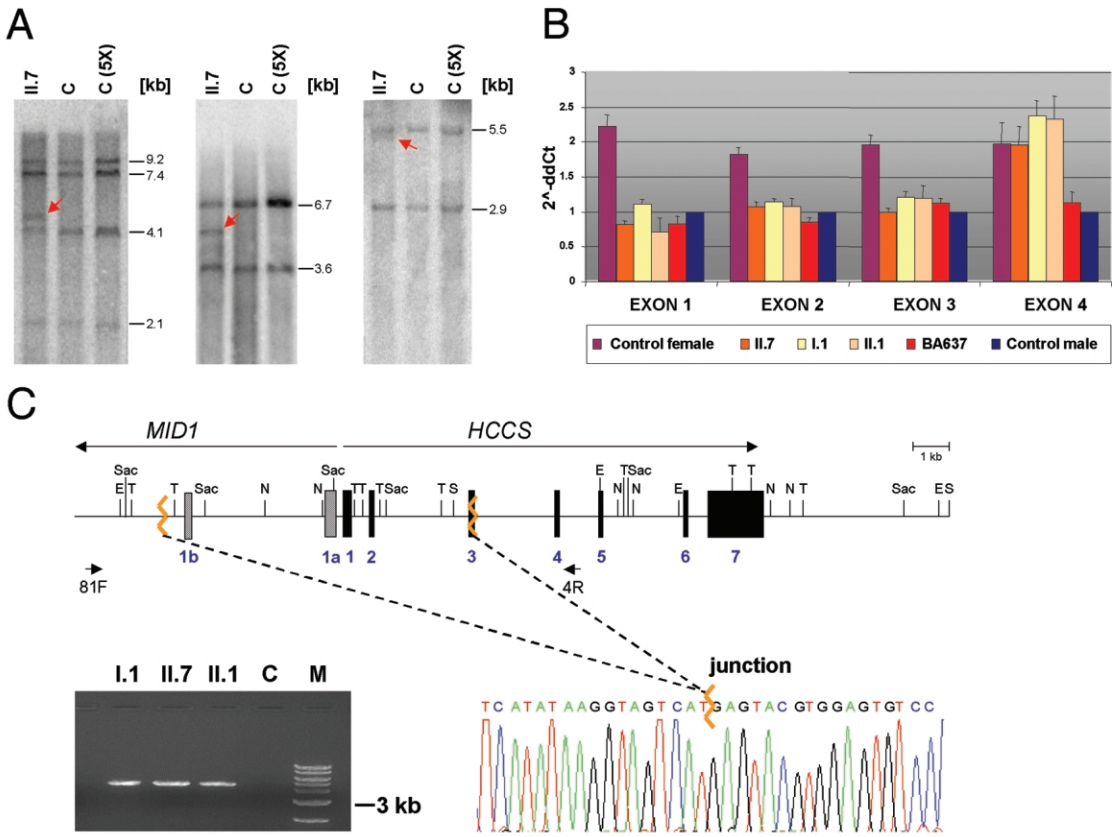

Figure 2. A submicroscopic deletion encompassing part of the *HCCS* gene is present in three members of the family of patient II.7. *A,* Southern blot hybridized with a probe covering the *HCCS* 5′ UTR and coding region. Genomic DNA samples of patient II.7 and controls were digested with *Spe*I and *Eco*RV (*left*), *Nde*I and *Sac*I (*middle*), and *Taq*I (*right*). C = female control; C (5X) = human cell line with five X chromosomes. Various fragments of altered sizes (*red arrows*) were observed in II.7. *B,* Relative quantification of copy numbers of *HCCS* exons 1–4, by real-time PCR on genomic DNA of individuals I.1, II.1, and II.7. BA637 has MLS and displays monosomy of the Xp22 region.[5] Values of *HCCS* exons 1–3 in II.7, II.1, and I.1 are comparable to that of a haploid sample. *C,* Schematic representation of part of the MLS critical region (*top*). *MID1* and *HCCS* genes are indicated by long arrows, and primers used for junction fragment amplification are indicated by short arrows. Exons 1a and 1b of *MID1* are represented by bars, exons of *HCCS* by black boxes. Jagged orange lines indicate deletion breakpoints. E = *Eco*RV; N = *Nde*I; S = *Spe*I; Sac = *Sac*I; T = *Taq*I. *Bottom left panel,* Amplification of a junction fragment from genomic DNA of I.1, II.1, and II.7 but not from a control (C). M = DNA marker. *Bottom right panel,* Part of the DNA sequence electropherogram of the rearrangement-specific junction fragment. The deletion breakpoint is indicated by a jagged orange line. The 8.6-kb deletion encompasses *HCCS* exons 1–2, part of exon 3, and exons 1a and 1b of *MID1*.

of a left diaphragmatic hernia. High-resolution karyotype of both affected sisters was normal.

Patient MS1, a 5-year-old girl, is the first child of healthy parents. Pregnancy was uneventful, and delivery was without any complication; birth measurements were in the upper-normal range. The newborn showed bilateral microphthalmia (more severe on the right), with bilateral cloudy and vascular cornea. In addition, linear and patchy erythrodermia of the patient's cheeks and right lateral neck was noticed immediately after birth. At age 3 mo, complete sclerocornea was noticed; however, erythrodermia had faded gradually. Reexamination at age 6 mo revealed poor vision but only very mild facial erythrodermia and only mild developmental delay. Cranial magnetic-resonance-imaging studies at age 1 year demonstrated hypoplasia of the corpus callosum, lack of the septum pellucidum, and slightly dilated third ventricle. The patient's further development was characterized by normal growth, mild-to-moderate developmental delay, and very severe visual impairment. The happy-natured girl is now able to speak short sentences.

Patient MS2, a 9-year-old girl, was born to healthy unrelated parents after an uneventful pregnancy. Birth measurements were within the normal range. After birth, she presented with bilateral microphthalmia and sclerocornea. A small mandible, a single palmar crease, and a sandal gap but no erythematous skin lesions were noticed. At the end of her 1st year of life, she developed idiopathic ventricular tachycardia, which was converted to normal sinus rhythm by amiodaron and ajmalin. After extubation and end of sedation, she suffered an occlusion of her right arteria cerebri media and subsequently developed hemiparesis on the left side. Neurologic symptoms declined after physiotherapy. At age 8 years, she suffered a sole tonic-clonic seizure.

Our ethics committees approved this study, and written informed consent was obtained from all participants or their legal guardians.

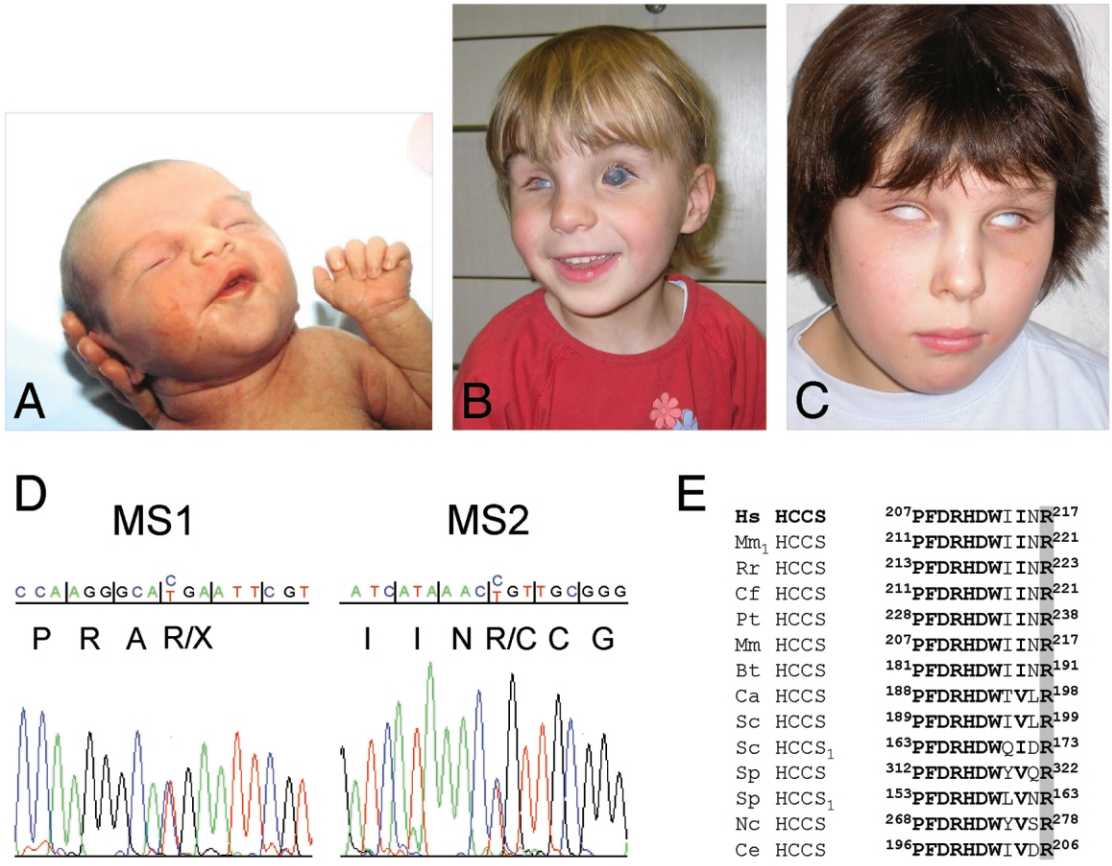

Figure 3. Point mutations in *HCCS* in two patients with MLS. *A–C,* Photographs of patients MS1 and MS2. *A,* Linear skin defects located on the face and neck of patient MS1 at birth. *B,* Microphthalmia of the right eye and bilateral sclerocornea of patient MS1 at age 4 years. Linear skin defects have completely disappeared. *C,* Patient MS2, at age 8 years, with bilateral microphthalmia and sclerocornea. No linear skin defects were noted at birth. *D,* Sequence electropherograms of part of *HCCS* exons from genomic DNA of patients MS1 and MS2. Nucleotide triplets and encoded amino acids are indicated. Patient MS1 is heterozygous for the c.589C→T mutation (p.R197X) (*left panel*) in exon 6, whereas the heterozygous mutation c.649C→T (p.R217C) (*right panel*) in exon 7 was found in patient MS2. *E,* Partial amino acid–sequence alignment of heme lyases from various species. The position of amino acids is given. Evolutionarily conserved residues are shown in bold. The invariant arginine at position 217, which is altered to cysteine in patient MS2, is shaded in gray. $HCCS_1$ indicates specificity of the heme lyase for cytochrome c_1. Hs = *Homo sapiens*; Mm_1 = *Mus musculus*; Rr = *Rattus norvegicus*; Cf = *Canis familiaris*; Pt = *Pan troglodytes*; Mm = *Macaca mulatta*; Bt = *Bos taurus*; Ca = *Candida albicans*; Sc = *S. cerevisiae*; Sp = *Schizosaccharomyces pombe*; Nc = *Neurospora crassa*; Ce = *Caenorhabditis elegans*.

Mutation Analysis, X-Inactivation Assay, and Real-Time PCR

Genomic DNA was isolated by standard procedures. We amplified the coding region (exons 2–7) of *HCCS* (GenBank accession number NM_005333), including the flanking intronic sequences, from genomic DNA. Primer sequences and PCR conditions are available on request. PCR products were directly sequenced with the Big Dye Terminator ready reaction kit (PE Applied Biosystems) on an ABI Prism 377 (PE Applied Biosystems).

Examination of the methylation pattern at the androgen receptor (*AR*) locus was performed according to the procedures of Allen et al.,[24] with minor modifications. For each DNA sample, two reactions were prepared: in the first, 400 ng of DNA was digested with 8 U *Hpa*II in a total volume of 10 μl, for 30 min at 37°C; in the second, 400 ng DNA was incubated with the enzyme reaction buffer, but without enzyme. To confirm complete digestion, DNA samples from a male and from a female with unilateral X inactivation were included as controls. Subsequent PCR amplification of the *AR* locus with primers AR-A_FAM (5′-CTTTCCAGAATCTGTTCCAG-3′; labeled with 5′ FAM) and AR-B (5′-AAGGTTGCTGTTCCTCATC-3′) was performed in a 25-μl reaction volume for 40 ng of the undigested DNA and in a total of 50 μl volume for 250 ng of *Hpa*II-cleaved DNA. The PCR contained both oligonucleotide primers at a concentration of 0.4 μM each, 0.2 mM dinucleotide triphosphates (dNTPs), and 0.5 U *Taq* polymerase (QIAGEN). Samples were denatured, with use of a PTC thermocycler (MJ Research), at 95°C for 3 min, followed by 35 cycles at 95°C for 1 min, at 55°C for 1 min, and at 72°C for 1 min, followed by a final incubation at 72°C for 10 min. A quantity of 0.4–0.8 μl of the amplicons was mixed with 20 μl deionized formamide and 0.4 μl TAMRA (red fluorescent dye) Size Standard (PE Applied Biosystems) and was denatured at 95°C for 5 min.

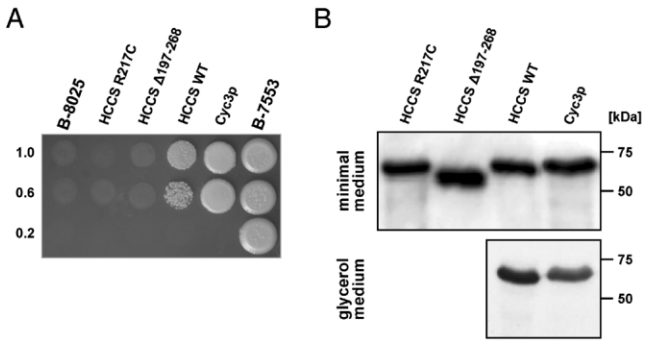

Figure 4. HCCS mutant proteins are not able to complement *S. cerevisiae CYC3* deficiency. *A,* Functional complementation of the *S. cerevisiae* strain B-8025. B-8025 was transformed with human wild-type HCCS (HCCS WT), the mutants Δ197–268 and R217C, or yeast CYC3 (Cyc3p) expression constructs and was grown on minimal medium. Transformants were grown in liquid minimal medium, and aliquots of 5 μl of saturated and diluted cultures were spotted on glycerol medium containing copper (to induce expression of GST-fusion proteins) and were incubated for 5 d at 30°C. The top row shows spots of saturated cultures, and the middle and bottom rows show spots of dilutions; dilution rates are indicated to the left of the figure. Note partial restoration of growth by Cyc3p and wild-type HCCS, whereas no growth was observed for the untransformed strain or that expressing HCCS Δ197–268 or HCCS R217C. In parallel, all strains were also spotted on plates with glucose-containing minimal medium and showed normal growth (data not shown). Strain B-7553 served as wild-type growth control. *B,* Expression of GST-HCCS–fusion proteins determined by western blotting. Expression of GST-HCCS R217C–, Δ197–268–, wild-type–, and GST-Cyc3p–fusion proteins in yeast strain B-8025, grown in minimal medium with copper, was demonstrated by immunoblotting (*top panel*), whereas, in strain B-8025 grown in glycerol-containing medium, only GST-HCCS wild-type– and GST-Cyc3p–fusion proteins were expressed (*lower panel*). B-8025 transformed with the GST-HCCS Δ197–268 or GST-HCCS R217C construct did not grow under this condition.

PCR products were analyzed on an ABI Prism 310 Genetic Analyzer (PE Applied Biosystems). Data were taken as a ratio of peak areas of the shorter-to-longer alleles.

Real-time quantitative PCR on genomic DNA was performed using an ABI Prism 7000 (PE Applied Biosystems) in a 96-well optical plate, with a final reaction of 20 μl. All reactions were prepared with 10 μl of 2× SYBR green I fluorescent dye PCR Master Mix and 400 nM forward and reverse primers. Primers for real-time experiments were designed using the Primer Express software, in accordance with the PE Applied Biosystems guidelines; primers sequences are available on request. The *RPP30* gene (GenBank accession number NM_006413) coding for a ribonuclease P was used as an internal reference. A total of 100 ng of DNA was used as a template for each sample; each was analyzed in quadruplicate. Thermal cycling conditions included a prerun of 2 min at 50°C and of 10 min at 95°C. Cycle conditions were 40 cycles at 95°C for 15 s and at 60°C for 1 min, in accordance with the PCR protocol (PE Applied Biosystems). Relative quantification of exon-copy numbers on genomic DNA was performed using the comparative threshold cycle (ddCt) method: the starting copy number of exons in patients was determined in comparison with the known copy number of the calibrator sample (healthy male control), with use of the formula

$$\begin{aligned} \text{ddCt} = {} & \text{dCt } \textit{HCCS} \text{ (patient with MLS)} \\ & - \text{dCt } \textit{RPP30} \text{ (patient with MLS)} \\ & - \text{dCt } \textit{HCCS} \text{ (healthy male)} \\ & - \text{dCt } \textit{RPP30} \text{ (healthy male)} \ . \end{aligned}$$

The relative exon-copy number was calculated by the expression $2^{\wedge} -$ (ddCt ± SE) that is of ~2 for a diploid sample and ~1 for a haploid sample.

Haplotype and SNP Analysis

Haplotype analysis of family members of patient II.7 was performed using five polymorphic microsatellite markers (tel-*DXS7108-CxM06-CxM09-DXS8019-DXS999*-cen) in the Xp22.2-p22.13 region, which contains the *HCCS* gene. PCR products were amplified using FAM (blue fluorescent)–labeled primers, following standard methods, and were electrophoresed on an ABI Prism 3100 Genetic Analyzer. Results were processed by GENESCAN software (PE Applied Biosystems).

For analysis of polymorphism *rs5901444,* exon 1 containing the trinucleotide CGG repeat was amplified using forward (5′-CCTGCCACCGCCACATTTTG-3′) and reverse (5′-ATGAATAGGA-ATTCGAAGAAACGAAGG-3′) primers. The PCR contained both primers, each at a concentration of 0.2 μM, 0.2 mM dNTPs, and 1 U AmpliTaq Gold (PE Applied Biosystems), in a total volume of 30 μl. Samples were amplified using a GeneAmp PCR System 9700 thermocycler (PE Applied Biosystems), with an initial denaturation at 95°C for 7 min and 35 cycles at 98°C for 1 min, at 58°C for 1 min, and at 72°C for 1 min.

RT-PCR

Total RNA was extracted from Epstein Barr virus–transformed lymphoblastoid cells of patient MS1 with the RNeasy kit (QIAGEN), according to the manufacturer's instructions. For first-strand cDNA synthesis, 1 μg of total RNA was reverse transcribed by using the Omniscript RT Kit (QIAGEN) and random hexamers, according to the protocol provided. Of each first-strand reaction, 1 μl cDNA was taken as template in PCRs, with use of Advantage cDNA-Polymerase Mix (BD Biosciences Clontech) and primers HCCS_RT_4F (5′-ATATCATTAGAATTCACAATCAG-3′) and HCCS_RT_3R (5′-AAACTGCAAGGTACAACACAAGTC-3′). The PCR condition was as follows: 35 cycles, each comprising 15 s at 95°C, 10 s at 58°C, and 40 s at 72°C, with an initial denaturation at 95°C for 3 min.

Southern-Blot Analysis

For Southern-blot analysis, 10 μg of genomic DNA was digested with the appropriate restriction enzymes: *Spe*I and *Eco*RV (double digestion), *Nde*I and *Sac*I (double digestion), and *Taq*I. DNA was separated by electrophoresis in 0.8% agarose gel, was transferred to Hybond-N (Amersham), and was hybridized to a probe covering the coding and the 5′ UTR regions of the *HCCS* transcript. This probe was generated by RT-PCR on cDNA obtained from lymphoblastoid cell lines, with use of primers RTF1 (5′-CGTGAA-

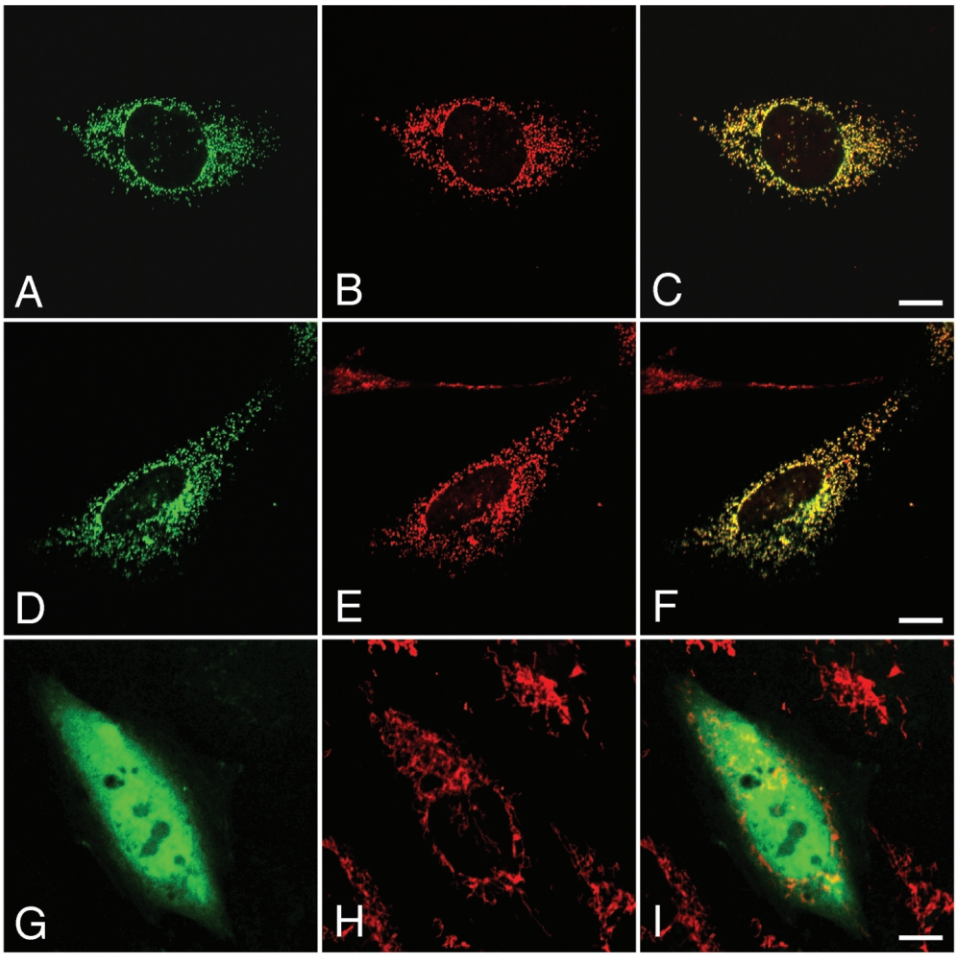

Figure 5. Targeting of ectopically expressed HCCS wild-type and mutant proteins to mitochondria. Subcellular localization of different N-terminally HA-tagged HCCS proteins ectopically expressed in CHO-K1 cells (*A, D,* and *G*) and staining of endogenous mitochondria by MitoTracker (*B, E,* and *H*) are shown. HA-tagged HCCS wild-type protein (*A* [*green*]) is targeted to mitochondria (*B* [*red*]), as shown by colocalization with the MitoTracker (*C* [*yellow*]). Similarly, HA-tagged HCCS R217C mutant protein (*D* [*green*]) shows a mitochondrial (*E* [*red*]) distribution (*F* [*yellow*]). In contrast, the truncated HCCS Δ197–268 protein is diffusively dispersed in the cell (*G*), and the two fluorescence patterns (*G* and *H*) show no overlap (*I*). The scale bars represent 10 μm.

GTCACTGCTGCTCTG-3′) and RTR1 (5′-TCTGAAACAGTGCTTT-ACGAGGTC-3′).

Generation of N- and C-Terminal–Tagged HCCS *Constructs*

HCCS cDNA clone DKFZp779I1858 (GenBank accession number CR749578) was provided by the RZPD German Resource Center for Genome Research (Berlin). The DNA insert of this cDNA clone was sequenced by SP6 and T7 primers and primer walking (primer sequences are available on request). Wild-type *HCCS* and *HCCS* (Δ197–268) cDNA inserts were generated using specific PCR primers and the DKFZp779I1858 clone as template. The *HCCS* (R217C) insert was established by PCR-mediated mutagenesis.[25] Purified PCR products were cloned into pENTR/D-TOPO (Invitrogen) according to the protocol provided. Constructs were sequenced for integrity and then were used for cloning the *HCCS*-coding region into plasmids pcDNA-DEST53 (N-terminal EGFP epitope [Invitrogen]), pcDNA-DEST47 (C-terminal EGFP epitope [Invitrogen]), pMT2SM-HA-DEST (N-terminal HA epitope), and pcDNA3.2/V5-DEST (C-terminal V5 epitope [Invitrogen]) via left-right reaction, following the manufacturer's instructions. Plasmid pMT2SM-HA-DEST was generated by blunt-end ligation of the GATEWAY Cloning Reading Frame Cassette C (Invitrogen) into the multiple cloning site of vector pMT2SM-HA.

Generation of Yeast-Expression Constructs

All yeast-expression constructs were generated in pYEX4Tps, which drives expression of the glutathione-S-transferase (GST)–fusion proteins from the *Saccharomyces cerevisiae* CUP1 promoter and carries the selectable markers *leu2-d, URA3,* and Amp^r. To generate pYEX4Tps-HCCS wild type and pYEX4Tps-HCCS Δ197–268, PCR products were amplified by using specific PCR primers and the DKFZp779I1858 clone as template. pYEX4Tps-HCCS-R217C was established by PCR-mediated mutagenesis.[25] After purification of PCR products, each amplicon was restricted with *Bam*HI and *Not*I and was cloned unidirectionally into pYEX4Tps. To establish the control construct pYEX4Tps-CYC3, a PCR product was amplified

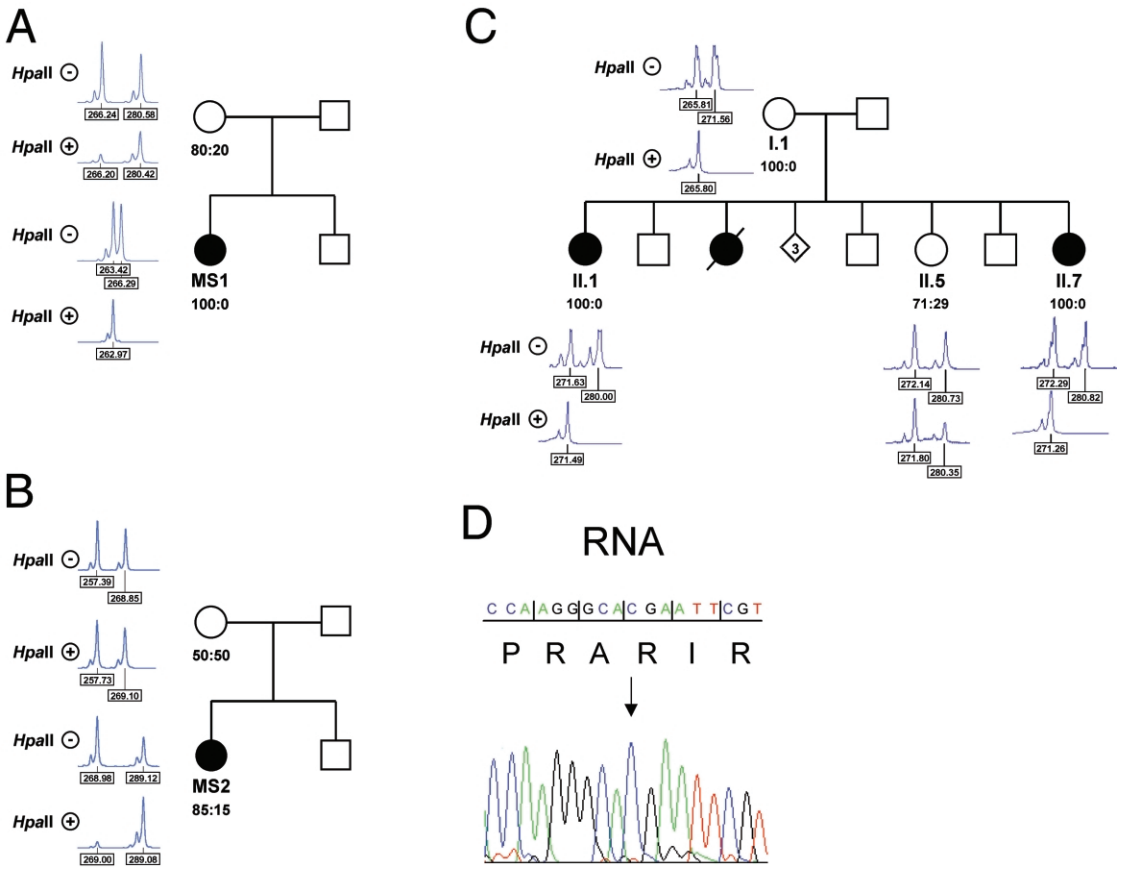

Figure 6. Skewed X inactivation in females with an *HCCS* mutation. X-chromosome inactivation determined by amplification of an *AR*-sequence polymorphism and digestion of genomic DNA isolated from lymphocytes with *Hpa*II (indicated with plus [+] and minus [−] signs, respectively). The ratio of the X-inactivation pattern is given below the respective pedigree symbol. All females carrying an *HCCS* mutation show nonrandom or extremely skewed X inactivation (patient MS1 in panel A; patient MS2 in panel B; and II.1, II.7, and their mother [I.1] in panel C). *D,* Part of the DNA sequence electropherogram of *HCCS* exon 6, obtained from an RT-PCR amplicon of patient MS1. Only the wild-type allele (c.589C) (*arrow*) is expressed in her lymphoblastoid cells.

by using specific primers and pAB256 carrying yeast *CYC3* as template. Subsequently, the amplicon was cloned as *Bam*HI-*Not*I fragment into pYEX4Tps. Primer sequences and PCR conditions are available on request. All constructs were sequenced for integrity, and large and pure amounts of plasmid DNA were prepared by using a plasmid maxikit (QIAGEN).

Immunofluorescence

CHO-K1 cells were cultured on fibronectin-coated (10 μg/ml) coverslips in F12-Ham's Nutrient Mixture supplemented with 10% fetal calf serum, 1% L-glutamine, and penicillin-streptomycin, at 37°C in 5% CO_2. Cells were transfected with pcDNA-DEST53-HCCS wild type, pcDNA-DEST53-HCCS R217C, pcDNA-DEST53-HCCS Δ197–268, pcDNA-DEST47-HCCS wild type, pcDNA-DEST47-HCCS R217C, pcDNA-DEST47-HCCS Δ197–268, pMT2SM-HA-DEST-HCCS wild type, pMT2SM-HA-DEST-HCCS R217C, pMT2SM-HA-DEST-HCCS Δ197–268, pcDNA3.2/V5-DEST-HCCS wild type, pcDNA3.2/V5-DEST-HCCS R217C, and pcDNA3.2/V5-DEST-HCCS Δ197–268 (each with 1 μg of DNA), with use of Lipofectamine 2000 reagent (Invitrogen) according to the manufacturer's protocol, and were incubated overnight. The next day, cells were incubated in normal growth medium supplemented with 50 nM MitoTracker Red CMXRos (Invitrogen) for 20 min at 37°C, were rinsed in PBS, and were fixed with 4% paraformaldehyde in PBS. After washing three times with PBS, EGFP-transfected cells on coverslips were directly mounted in glycerol gelatin (Sigma). Cells transfected with HA- or V5-tagged *HCCS* constructs were incubated in permeabilization/blocking solution (2% BSA, 3% goat serum, and 0.5% Nonidet P-40 in PBS) for 60 min. Subsequently, HA- and V5-tagged HCCS proteins were detected with rat monoclonal anti-HA-Flourescein antibody (1.25 μg/ml) (Roche) and mouse monoclonal anti-V5-FITC antibody (2.0 μg/ml) (Invitrogen), respectively, both diluted in antibody solution (3% goat serum and 0.1% Nonidet P-40 in 1× PBS). After extensive washing with PBS, cells were mounted in glycerol gelatin on microscopic slides. Images were acquired with use of a Zeiss Axiovert 200 M confocal microscope equipped with a 63× Planapochromat/1.4 DIC lens.

Yeast-Complementation Studies

For complementation studies, we used *S. cerevisiae* strain B-8025 (MATα *can1-100 CYC1 cyc3-Δ cyc7-Δ::CYH2 cyh2 his3-Δ1 leu2-3,112 trp1-289*), which carries a deletion of *CYC3*,[26] as well as B-

7553 (MATα *can1-100 CYC1 cyc7::CYH2 cyh2 his3-Δ1 leu2-3,112 trp1-289*) as a growth control.[27] Both B-8025 and B-7553 carry a deletion of *CYC7,* which encodes cytochrome c_1, one of the two yeast cytochrome *c* proteins. Strains lacking *CYC3* but still harboring *CYC7* may still show residual respiratory growth due to conversion of apocytochrome c_1 to its holoform by the second yeast heme lyase Cyt2p. Thus, the *CYC3*$^-$ mutant strain lacking *CYC7* is not able to grow at all on nonfermentable carbon sources and needs complementation to show respiratory growth.

Yeast cells were maintained in complete medium (YPD). Transformation of cells was done by the standard lithium-acetate method. Positive transformants were selected by growth in minimal medium, supplemented with 2% glucose but lacking leucine. Colonies that showed growth under this condition were grown in liquid minimal medium until saturation and subsequently were tested for growth on nonfermentable carbon sources (YPG medium containing 3% glycerol, 2% peptone, 1% yeast extract, 2% agar, and 0.2 mM $CuSO_4$). Therefore, we generated two dilutions (0.6-fold and 0.2-fold) from a saturated culture of each strain and spotted 5 μl of these cultures on YPG plates and in parallel, as growth control, on plates containing minimal medium with glucose. Plates were incubated for 5 d at 30°C.

Immunoblotting

Expression of various GST-HCCS and GST-CYC3–fusion proteins was confirmed by immunoblotting of lysates from saturated yeast cultures (grown in minimal medium or YPG medium with copper) with use of horseradish peroxidase–conjugated goat polyclonal anti-GST antibody (0.3 μg/ml) (Amersham Pharmacia Biotech).

Results

We examined a family in which the youngest daughter (II.7) shows the classic MLS phenotype and a normal karyotype. However, a pathogenic mutation in *MID1, ARHGAP6,* and *HCCS* in patient II.7 has not yet been identified.[5] The older sister (II.1) presents a milder phenotype, a third affected daughter (II.3) died at age 6 h, and three spontaneous abortions were also reported (fig. 1*B*). The mother has no obvious signs of MLS, although we cannot exclude the presence of skin lesions early in infancy that disappeared over time; the examination with a UV light was not possible. In an attempt to find a microdeletion within the MLS critical region, we performed segregation analysis using polymorphic markers within the *HCCS* gene (CGG repeat of SNP *rs5901444*) and from regions nearby (*DXS7108, CxM06, CxM09, DXS8019,* and *DXS999*). For SNP *rs5901444,* which is located in the 5′ UTR of *HCCS,* the mother carries seven CGG repeats, whereas the father has eight (fig. 1*B*). Remarkably, both patients (II.7 and II.1) carry only the paternal allele with eight CGG repeats, which suggests that the mother is hemizygous rather than homozygous for this repeat (fig. 1*B*). Segregation analysis showed that the two affected individuals carry a different maternal haplotype than do their four unaffected siblings (fig. 1*B*). To identify a submicroscopic deletion, we performed Southern-blot analysis with cDNA probes complementary to the *HCCS* 5′ UTR and coding region, using genomic DNA of patient II.7 digested with various enzymes. In addition to the expected pattern, we identified aberrant bands in the patient compared with control samples, which suggests the presence of a heterozygous cryptic rearrangement involving the *HCCS* gene (fig. 2*A*). We used real-time PCR for comparative quantification of copy numbers of *HCCS* exon 1–7 amplicons on genomic DNA of patient II.7, her sister (II.1), and the asymptomatic mother (I.1). The relative copy number of *HCCS* exons 1–3 was comparable to a haploid sample, whereas that of exons 4–7 was comparable to a diploid sample in the three females (fig. 2*B*). We subsequently amplified a 4,764-bp breakpoint-spanning PCR product from the DNA of patients II.1 and II.7 and their mother (fig. 2*C*). Direct sequencing of the junction fragment revealed the presence of an 8.6-kb deletion comprising *HCCS* exons 1 and 2, the first 83 bp of exon 3, the 5′ untranslated exons 1a and 1b of *MID1,* as well as the respective intronic sequences in I.1, II.1, and II.7 (fig. 2*C*). This deletion was absent in the three males (II.2, II.4, and II.6) and in the unaffected female sibling (II.5) of the proband (data not shown). In summary, we found no evidence of the presence of a mosaicism in the mother as explanation of her phenotype.

The identification of a microdeletion makes *HCCS* a strong candidate gene for MLS. Therefore, we studied two previously unreported female patients with MLS: 5-year-old patient MS1 and 9-year-old patient MS2 (fig. 3*A*–3*C*), who both carry an apparently normal female karyotype. By sequence analysis of the coding regions and exon-intron boundaries of *HCCS,* we identified a heterozygous c.589C→T (p.R197X) mutation in exon 6 of patient MS1, as well as a heterozygous c.649C→T (p.R217C) mutation in exon 7 of patient MS2 (fig. 3*D*). The mutations were found neither in the parents (paternity confirmed) nor in 50 (for c.589C→T) or 110 (for c.649C→T) female controls (data not shown). The ethnicity of the controls matched that of the patients. The mutation found in patient MS2 affects the arginine residue at position 217 of the HCCS protein, which is highly conserved across evolution in all heme lyases,[28] suggesting an important function of this amino acid (fig. 3*E*). In contrast, the sequence change in patient MS1 causes a premature stop located 21 nt upstream of the last splicing-generated exon-exon junction, which may define either a functional null allele due to nonsense-mediated mRNA decay (NMD) or an HCCS protein lacking 72 C-terminal amino acids (Δ197–268). The latter assumption is more likely, since mRNAs with premature termination codons located <50–55 nt upstream of the most 3′ exon-exon junction are generally not targeted for NMD.[29]

The *S. cerevisiae* strain B-8025 shows a severely depleted respiratory function and is unable to grow on nonfermentable carbon sources because of deletion of *CYC3,* which encodes the yeast orthologue of the cytochrome *c* heme lyase (Cyc3p).[30] This deficiency has been shown to be complemented by ectopically expressed human HCCS protein.[12] We expressed various human HCCS and yeast

Cyc3 proteins as GST-fusion proteins in yeast strain B-8025 and analyzed their capacity to compensate for respiratory deficiency. As expected, wild-type human HCCS and yeast Cyc3 proteins were able to restore growth on glycerol-containing medium. Notably, complementation by yeast Cyc3p is only partial; that is probably because of expression of a GST-fused protein. In contrast, expression of either the C-terminally truncated HCCS protein (Δ197–268) or HCCS carrying the missense mutation p.R217C does not restore growth (fig. 4*A*). By western-blot analysis of protein extracts from the transformed B-8025 strains grown in minimal medium, we confirmed expression of the four GST-fusion proteins: human wild-type HCCS, Δ197–268, R217C, and yeast Cyc3p (fig. 4*B*).

To investigate whether the mutated HCCS proteins are still directed to mitochondria, we compared subcellular localization of ectopically expressed wild-type HCCS with mutated HCCS proteins. Indeed, we observed that N-terminally HA-tagged wild-type HCCS protein is localized to mitochondria in CHO-K1 cells (fig. 5*A*–5*C*). Similarly, ectopically expressed HCCS with cysteine-217 (HCCS R217C) is also targeted to mitochondria (fig. 5*D*–5*F*), whereas the HCCS mutant protein Δ197–268 was dispersed in the cytoplasm and nucleus (fig. 5*G*–5*I*). We obtained similar results with wild-type HCCS proteins and the two mutants carrying an N- or C-terminal EGFP tag or a C-terminal V5 tag (data not shown).

The *HCCS* gene product is supposed to act in a cell-autonomous manner; therefore, functional nullisomy should result in selective cell loss and consequent nonrandom X inactivation in various tissues of heterozygous females. We used the methylation-specific PCR at the polymorphic human *AR* locus to study the X-inactivation pattern in all females carrying an *HCCS* mutation. In patients MS1, MS2, II.7, the sister of II.7 (II.2), and the mother of II.7 and II.2 (I.1), a skewed X chromosome–inactivation pattern (85%–100%) in peripheral-blood cells was found (fig. 6*A*–6*C*). Consistently, a skewed X inactivation was also observed in buccal mucosa cells of patient MS1, as well as in fibroblasts of patient II.7 (data not shown). Results from the X-inactivation studies for patients II.1 and II.7 suggest that there is a selective disadvantage for cells carrying the active maternal X chromosome (fig. 6*C*). Moreover, in both MS1 and MS2, the paternal X chromosome was found to be preferentially inactivated (fig. 6*A* and 6*B*). Accordingly, by RT-PCR analysis, we showed that only *HCCS* mRNA transcribed from the wild-type allele is detected in lymphoblastoid cells of patient MS1 (carrying p.R197X), suggesting that the nonsense mutation occurred on the paternal allele (fig. 6*D*).

Discussion

The findings that (1) *HCCS* maps within the smallest MLS critical region—that is, *HCCS* is deleted in all patients carrying chromosomal abnormalities, (2) *HCCS* is partially deleted in two sisters with MLS and their asymptomatic mother, and (3) loss-of-function point mutations occurred de novo in two patients with MLS provide strong evidence of the involvement of the holocytochrome *c*–type synthase in the pathogenesis of this syndrome. Thus, absence of heme-lyase activity in hemizygous human males is most likely the cause of their in utero lethality. Similarly, in vivo–generated deletions involving the equivalent critical MLS region in the mouse (MLS^{Δ}), encompassing *Hccs* as well as parts of *Mid1* and *Arhgap6,* lead to lethality of hemizygous, homozygous, and heterozygous embryos early in development. This lethality can be rescued by overexpression of the human *HCCS* gene from a BAC clone, providing proof that lethality is indeed due to loss of *HCCS*.[31] Clearly, MLS belongs to the group of X-linked dominant male-lethal disorders, including, for example, incontinentia pigmenti and chondrodysplasia punctata 2.[22]

Functional analysis of both the nonsense (p.R197X) and the missense (p.R217C) mutations revealed that (1) the 72 C-terminal amino acids are required for mitochondrial targeting and (2) arginine-217 seems to be necessary for proper function of HCCS. Consistently, an evolutionarily conserved motif located within residues 190–216 of human HCCS was shown to be important for sorting of heme lyases to the intermembrane space of mitochondria.[28] The arginine residue at position 217 is an invariant amino acid in all HCCS proteins and is located next to one of the two internal targeting signals (aa 190–216),[28] which suggests an important role of this residue for the integrity of the holocytochrome *c*–type synthase.

Dysfunction of assembly factors of the mitochondrial respiratory chain, such as the holocytochrome *c*–type synthase, are known to cause various conditions with typical symptoms of mitochondrial diseases, including myopathy, encephalomyopathy, or cardiomyopathy, with a variable age at disease onset.[32,33] However, the data presented here show, for the first time (to our knowledge), that deficiency of a mitochondrial housekeeping enzyme implicated in OXPHOS may also cause a severe developmental disorder with microphthalmia, sclerocornea, and areas of aplastic skin. Thus, the complex phenotype of females with MLS raises the question of a possible second function of HCCS or its final product that is not directly related to OXPHOS.

The holocytochrome *c*–type synthase or heme lyase is located at the outer surface of the inner mitochondrial membrane and catalyzes the covalent attachment of heme to apocytochrome *c* (and c_1), which leads to the mature holocytochrome *c*.[30,34] In *S. cerevisiae,* two heme lyases exist, the cytochrome *c*- (Cyc3p) and the cytochrome c_1-specific heme lyase (Cyt2p), whereas only a single heme lyase is required for maturation of both cytochrome *c* and c_1 in higher eukaryotes.[11,13] Defects in either of the yeast heme lyases result in loss of respiratory growth of the respective strain.[30,34]

Cytochrome *c* is released from mitochondria in response to a variety of intrinsic death-promoting stimuli, thereby

leading to caspase-dependent death or apoptosis.[15] Subsequent binding of cytochrome *c* to the apoptotic protease-activating factor 1 (APAF-1) and the recruitment and activation of procaspase-9 cleaves other caspases to execute apoptosis.[35] Mice deficient for cytochrome *c* as well as knock-in mice expressing a mutant cytochrome *c,* which retains its normal electron transfer function but is unable to activate APAF-1, die perinatally because of severe developmental defects. Cells derived from both mice show defects in apoptosis, because they are unable to form the active apoptosome.[36,37] Apoptosis is important for proper neuronal development—for example, normal eye and brain development and impaired programmed cell death can lead to severe developmental defects in human and/or mouse.[38–42] In the same line, a mutant strain of *S. cerevisiae* lacking the cytochrome *c*–specific heme lyase Cyc3p is more resistant to death than the wild type,[43] which suggests that the mature form of cytochrome *c* is required for programmed cell death in yeast. Indeed, accumulation of apocytochrome *c* in the cytosol eukaryotic cells has been shown to cause inhibition of caspase-mediated apoptosis.[44] Together, these data suggest that the release of mature cytochrome *c* is important for programmed cell death, both in eukaryotic cells and in yeast. Accordingly, loss-of-function mutations of *HCCS* in human are not only supposed to give rise to severe functional deficits in OXPHOS in cells and tissues that rely mainly on mitochondrial energy supply, but they may also cause severe constraints in the process of apoptosis. However, elimination of key components of the intrinsic apoptotic cascade will not prevent cell death, since caspase-independent or nonapoptotic death—namely apoptosis-like death, autophagic cell death, or necrosis—can still occur.[45] Thus, absence of components forming the apoptosome, such as cytochrome *c,* will possibly result in a switch from apoptosis to selective cell loss with a necrotic morphology.[46] This type of caspase-independent cell death is characterized by loss of the mitochondrial transmembrane potential, low intracellular ATP concentrations, and generation of reactive oxygen species that occurred on disruption of the mitochondrial electron-transport chain.[47–50] Remarkably, necrosis has even been found to substitute for caspase-dependent apoptosis during embryonic development.[51,52] Thus, we speculate that the majority of cells lacking a functional copy of *HCCS* in heterozygous females will die because of severe defects in OXPHOS. Nonetheless, mitochondrial dysfunction and the resulting ATP depletion, along with lack of holocytochrome *c,* which is required to form the apoptosome, may push *HCCS*-deficient cells toward necrosis. It is of note that cell demise by necrosis bears the danger of provoking a chronic chain reaction of inflammation, with substantial damage to neighboring cells.[53,54]

In conclusion, our data show, for the first time, that mutations in *HCCS* are associated with the MLS phenotype. Implication of cytochrome *c*—the final HCCS product—in both OXPHOS and caspase-dependent apoptosis suggests that disturbance of the balance between necrosis and apoptosis may be a key element in the development of MLS symptoms in affected females. Further studies are required for better understanding of the contribution of pathogenic *HCCS* mutations and the individual pattern of X inactivation in the development of MLS.

Acknowledgments

We are grateful to the patients and their parents. We thank Cordula Steglich and Karin Ziegler, for skillful technical assistance; Thomas Rau, for help with confocal microscopy; Birgit Wiltschi (MPI Biochemie, Martinsried, Germany), for kindly providing plasmid pYEX4Tps; and Jaclyn Renfrow and Fred Sherman (both from Department of Biochemistry and Biophysics, University of Rochester Medical School, Rochester, NY), for yeast strains B-8025 and B-7553, as well as plasmids pAB268, pAB256, and pAB790. We also thank Annick Raas-Rothschild (Department of Human Genetics, Hadassah University Hospital, Jerusalem) for the characterization of patient II.7 and helpful discussion. This work was supported by grants from the Wilhelm-Sander-Stiftung (2003.160.1) (to K.K.) and the Telethon Foundation (to B.F.).

Web Resources

Accession numbers and URLs for data presented herein are as follows:

GenBank, http://www.ncbi.nlm.nih.gov/Genbank/ (for *HCCS* [accession number NM_005333], *RPP30* [accession number NM_006413], and *HCCS* cDNA clone DKFZp779I1858 [accession number CR749578])

Online Mendelian Inheritance in Man (OMIM), http://www.ncbi.nlm.nih.gov/Omim/ (for MLS phenotypes)

RZPD German Resource Center for Genome Research, http://www.rzpd.de/

References

1. Van den Veyver IB (2002) Microphthalmia with linear skin defects (MLS), Aicardi, and Goltz syndromes: are they related X-linked dominant male-lethal disorders? Cytogenet Genome Res 99:289–296
2. Bird LM, Krous HF, Eichenfield LF, Swalwell CI, Jones MC (1994) Female infant with oncocytic cardiomyopathy and microphthalmia with linear skin defects (MLS): a clue to the pathogenesis of oncocytic cardiomyopathy? Am J Med Genet 53: 141–148
3. Happle R, Daniels O, Koopman RJ (1993) MIDAS syndrome (microphthalmia, dermal aplasia, and sclerocornea): an X-linked phenotype distinct from Goltz syndrome. Am J Med Genet 47:710–713
4. Kherbaoui-Redouani L, Eschard C, Bednarek N, Morville P (2003) [Cutaneous aplasia, non compaction of the left ventricle and severe cardiac arrhythmia: a new case of MLS syndrome (microphthalmia with linear skin defects)]. Arch Pediatr 10:224–226
5. Morleo M, Pramparo T, Perone L, Gregato G, Le Caignec C, Mueller RF, Ogata T, Raas-Rothschild A, de Blois MC, Wilson LC, Zaidman G, Zuffardi O, Ballabio A, Franco B (2005) Microphthalmia with linear skin defects (MLS) syndrome: clin-

ical, cytogenetic, and molecular characterization of 11 cases. Am J Med Genet A 137:190–198
6. Zvulunov A, Kachko L, Manor E, Shinwell E, Carmi R (1998) Reticulolinear aplasia cutis congenita of the face and neck: a distinctive cutaneous manifestation in several syndromes linked to Xp22. Br J Dermatol 138:1046–1052
7. Wapenaar MC, Schiaffino MV, Bassi MT, Schaefer L, Chinault AC, Zoghbi HY, Ballabio A (1994) A YAC-based binning strategy facilitating the rapid assembly of cosmid contigs: 1.6 Mb of overlapping cosmids in Xp22. Hum Mol Genet 3:1155–1161
8. Quaderi NA, Schweiger S, Gaudenz K, Franco B, Rugarli EI, Berger W, Feldman GJ, Volta M, Andolfi G, Gilgenkrantz S, Marion RW, Hennekam RC, Opitz JM, Muenke M, Ropers HH, Ballabio A (1997) Opitz G/BBB syndrome, a defect of midline development, is due to mutations in a new RING finger gene on Xp22. Nat Genet 17:285–291
9. Schaefer L, Prakash S, Zoghbi HY (1997) Cloning and characterization of a novel rho-type GTPase-activating protein gene (*ARHGAP6*) from the critical region for microphthalmia with linear skin defects. Genomics 46:268–277
10. Prakash SK, Paylor R, Jenna S, Lamarche-Vane N, Armstrong DL, Xu B, Mancini MA, Zoghbi HY (2000) Functional analysis of ARHGAP6, a novel GTPase-activating protein for RhoA. Hum Mol Genet 9:477–488
11. Schaefer L, Ballabio A, Zoghbi HY (1996) Cloning and characterization of a putative human holocytochrome c-type synthetase gene (*HCCS*) isolated from the critical region for microphthalmia with linear skin defects (MLS). Genomics 34: 166–172
12. Schwarz QP, Cox TC (2002) Complementation of a yeast *CYC3* deficiency identifies an X-linked mammalian activator of apocytochrome c. Genomics 79:51–57
13. Bernard DG, Gabilly ST, Dujardin G, Merchant S, Hamel PP (2003) Overlapping specificities of the mitochondrial cytochrome *c* and c_1 heme lyases. J Biol Chem 278:49732–49742
14. Moraes CT, Diaz F, Barrientos A (2004) Defects in the biosynthesis of mitochondrial heme *c* and heme *a* in yeast and mammals. Biochim Biophys Acta 1659:153–159
15. Jiang X, Wang X (2004) Cytochrome *c*-mediated apoptosis. Annu Rev Biochem 73:87–106
16. Allanson J, Richter S (1991) Linear skin defects and congenital microphthalmia: a new syndrome at Xp22.2. J Med Genet 28:143–144
17. Kutsche K, Werner W, Bartsch O, von der Wense A, Meinecke P, Gal A (2002) Microphthalmia with linear skin defects syndrome (MLS): a male with a mosaic paracentric inversion of Xp. Cytogenet Genome Res 99:297–302
18. Lindsay EA, Grillo A, Ferrero GB, Roth EJ, Magenis E, Grompe M, Hulten M, Gould C, Baldini A, Zoghbi HY, Ballabio A (1994) Microphthalmia with linear skin defects (MLS) syndrome: clinical, cytogenetic, and molecular characterization. Am J Med Genet 49:229–234
19. Cape CJ, Zaidman GW, Beck AD, Kaufman AH (2004) Phenotypic variation in ophthalmic manifestations of MIDAS syndrome (microphthalmia, dermal aplasia, and sclerocornea). Arch Ophthalmol 122:1070–1074
20. Kobayashi M, Kiyosawa M, Toyoura T, Tokoro T (1998) An XX male with microphthalmos and sclerocornea. J Pediatr Ophthalmol Strabismus 35:122–124
21. Kono T, Migita T, Koyama S, Seki I (1999) Another observation of microphthalmia in an XX male: microphthalmia with linear skin defects syndrome without linear skin lesions. J Hum Genet 44:63–68
22. Franco B, Ballabio A (2006) X-inactivation and human disease: X-linked dominant male-lethal disorders. Curr Opin Genet Dev 16:254–259
23. Van den Veyver IB (2001) Skewed X inactivation in X-linked disorders. Semin Reprod Med 19:183–191
24. Allen RC, Zoghbi HY, Moseley AB, Rosenblatt HM, Belmont JW (1992) Methylation of *Hpa*II and *Hha*I sites near the polymorphic CAG repeat in the human androgen-receptor gene correlates with X chromosome inactivation. Am J Hum Genet 51:1229–1239
25. Ito W, Ishiguro H, Kurosawa Y (1991) A general method for introducing a series of mutations into cloned DNA using the polymerase chain reaction. Gene 102:67–70
26. Tong J, Margoliash E (1998) Cytochrome *c* heme lyase activity of yeast mitochondria. J Biol Chem 273:25695–25702
27. Dumont ME, Schlichter JB, Cardillo TS, Hayes MK, Bethlendy G, Sherman F (1993) *CYC2* encodes a factor involved in mitochondrial import of yeast cytochrome c. Mol Cell Biol 13: 6442–6451
28. Diekert K, Kispal G, Guiard B, Lill R (1999) An internal targeting signal directing proteins into the mitochondrial intermembrane space. Proc Natl Acad Sci USA 96:11752–11757
29. Nagy E, Maquat LE (1998) A rule for termination-codon position within intron-containing genes: when nonsense affects RNA abundance. Trends Biochem Sci 23:198–199
30. Dumont ME, Ernst JF, Hampsey DM, Sherman F (1987) Identification and sequence of the gene encoding cytochrome *c* heme lyase in the yeast *Saccharomyces cerevisiae*. EMBO J 6: 235–241
31. Prakash SK, Cormier TA, McCall AE, Garcia JJ, Sierra R, Haupt B, Zoghbi HY, Van Den Veyver IB (2002) Loss of holocytochrome *c*-type synthetase causes the male lethality of X-linked dominant microphthalmia with linear skin defects (MLS) syndrome. Hum Mol Genet 11:3237–3248
32. Shoubridge EA (2001) Nuclear genetic defects of oxidative phosphorylation. Hum Mol Genet 10:2277–2284
33. Zeviani M, Di Donato S (2004) Mitochondrial disorders. Brain 127:2153–2172
34. Dumont ME, Cardillo TS, Hayes MK, Sherman F (1991) Role of cytochrome *c* heme lyase in mitochondrial import and accumulation of cytochrome *c* in *Saccharomyces cerevisiae*. Mol Cell Biol 11:5487–5496
35. Hengartner MO (2000) The biochemistry of apoptosis. Nature 407:770–776
36. Hao Z, Duncan GS, Chang CC, Elia A, Fang M, Wakeham A, Okada H, Calzascia T, Jang Y, You-Ten A, Yeh WC, Ohashi P, Wang X, Mak TW (2005) Specific ablation of the apoptotic functions of cytochrome *c* reveals a differential requirement for cytochrome *c* and Apaf-1 in apoptosis. Cell 121:579–591
37. Li K, Li Y, Shelton JM, Richardson JA, Spencer E, Chen ZJ, Wang X, Williams RS (2000) Cytochrome *c* deficiency causes embryonic lethality and attenuates stress-induced apoptosis. Cell 101:389–399
38. Boya P, de la Rosa EJ (2005) Cell death in early neural life. Birth Defects Res C Embryo Today 75:281–293
39. de la Rosa EJ, de Pablo F (2000) Cell death in early neural development: beyond the neurotrophic theory. Trends Neurosci 23:454–458
40. Laemle LK, Puszkarczuk M, Feinberg RN (1999) Apoptosis in

early ocular morphogenesis in the mouse. Brain Res Dev Brain Res 112:129–133
41. Schafer ZT, Kornbluth S (2006) The apoptosome: physiological, developmental, and pathological modes of regulation. Dev Cell 10:549–561
42. Zeiss CJ (2003) The apoptosis-necrosis continuum: insights from genetically altered mice. Vet Pathol 40:481–495
43. Ludovico P, Rodrigues F, Almeida A, Silva MT, Barrientos A, Corte-Real M (2002) Cytochrome *c* release and mitochondria involvement in programmed cell death induced by acetic acid in *Saccharomyces cerevisiae*. Mol Biol Cell 13:2598–2606
44. Martin AG, Fearnhead HO (2002) Apocytochrome *c* blocks caspase-9 activation and Bax-induced apoptosis. J Biol Chem 277:50834–50841
45. Kroemer G, Martin SJ (2005) Caspase-independent cell death. Nat Med 11:725–730
46. Leist M, Jaattela M (2001) Four deaths and a funeral: from caspases to alternative mechanisms. Nat Rev Mol Cell Biol 2: 589–598
47. Bras M, Queenan B, Susin SA (2005) Programmed cell death via mitochondria: different modes of dying. Biochemistry (Mosc) 70:231–239
48. Leist M, Single B, Castoldi AF, Kuhnle S, Nicotera P (1997) Intracellular adenosine triphosphate (ATP) concentration: a switch in the decision between apoptosis and necrosis. J Exp Med 185:1481–1486
49. Nicotera P (2002) Apoptosis and age-related disorders: role of caspase-dependent and caspase-independent pathways. Toxicol Lett 127:189–195
50. Nicotera P, Melino G (2004) Regulation of the apoptosis-necrosis switch. Oncogene 23:2757–2765
51. Chautan M, Chazal G, Cecconi F, Gruss P, Golstein P (1999) Interdigital cell death can occur through a necrotic and caspase-independent pathway. Curr Biol 9:967–970
52. Oppenheim RW, Flavell RA, Vinsant S, Prevette D, Kuan CY, Rakic P (2001) Programmed cell death of developing mammalian neurons after genetic deletion of caspases. J Neurosci 21:4752–4760
53. Majno G, Joris I (1995) Apoptosis, oncosis, and necrosis. An overview of cell death. Am J Pathol 146:3–15
54. Proskuryakov SY, Konoplyannikov AG, Gabai VL (2003) Necrosis: a specific form of programmed cell death? Exp Cell Res 283:1–16